Biochimica et Biophysica Acta 1808 (2011) 352–359

Contents lists available at ScienceDirect

Biochimica et Biophysica Acta

journal homepage: www.elsevier.com/locate/bbamem

# Apolipoprotein E LDL receptor-binding domain-containing high-density lipoprotein: A nanovehicle to transport curcumin, an antioxidant and anti-amyloid bioflavonoid

Panupon Khumsupan [a], Ricardo Ramirez [a], Darin Khumsupan [a], Vasanthy Narayanaswami [a,b,*]

[a] Department of Chemistry and Biochemistry, 1250 Bellflower Boulevard, California State University Long Beach, Long Beach, CA 90840, USA
[b] Children's Hospital Oakland Research Institute, Oakland, CA 98609, USA

ARTICLE INFO

*Article history:*
Received 30 June 2010
Received in revised form 10 September 2010
Accepted 13 September 2010
Available online 17 September 2010

*Keywords:*
Apolipoprotein E
High density lipoprotein
Curcumin
Nanovehicle
Alzheimer's disease
Anti-amyloid
Nanodisc
Fluorescence

ABSTRACT

Curcumin is an antioxidant and anti-inflammatory bioflavonoid that has been recently identified as an anti-amyloid agent as well. To make it more available in its potent form as a potential amyloid disaggregation agent, we employed high-density lipoproteins (HDL), which are lipid–protein complexes that transport plasma cholesterol, to transport curcumin. The objective of this study was to employ reconstituted HDL containing human apoE3 N-terminal (NT) domain, as a vehicle to transport curcumin. The NT domain serves as a ligand to mediate binding and uptake of lipoprotein complexes via the low-density lipoprotein receptor (LDLr) family of proteins located at the cell surface. Reconstituted HDL was prepared with phospholipids and recombinant apoE3-NT domain in the absence or presence of curcumin. Non-denaturing polyacrylamide gel electrophoresis indicated that the molecular mass and Stokes' diameter of HDL bearing curcumin were ~670 kDa and ~17 nm, respectively, while electron microscopy revealed the presence of discoidal particles. Fluorescence emission spectra of HDL bearing (the intrinsically fluorescent) curcumin indicated that the wavelength of maximal fluorescence emission ($\lambda_{max}$) of curcumin was ~495 nm, which is highly blue-shifted compared to $\lambda_{max}$ of curcumin in solvents of varying polarity ($\lambda_{max}$ ranging from 515–575 nm) or in aqueous buffers. In addition, an enormous enhancement in fluorescence emission intensity was noted in curcumin-containing HDL compared to curcumin in aqueous buffers. Curcumin fluorescence emission was quenched to a significant extent by lipid-based quenchers but not by aqueous quenchers. These observations indicate that curcumin has partitioned efficiently into the hydrophobic milieu of the phospholipid bilayer of HDL. Functional assays indicated that the LDLr-binding ability of curcumin-containing HDL with apoE3-NT is similar to that of HDL without curcumin. Taken together, we report that apoE-containing HDL has a tremendous potential as a 'nanovehicle' with a homing device to transport curcumin to target sites.



## 1. Introduction

Curcumin (diferuloylmethane) is a polyphenolic phytochemical derived from the rhizome of *Curcuma* species, Zingiberaceae. It has been under intense scrutiny over the past two decades for its potent antioxidant, anti-inflammatory and cancer chemopreventive properties [1,2]. In addition, recent studies indicate a role for curcumin as a potential anti-amyloid agent due to its ability to inhibit amyloid beta peptide (Aβ) oligomerization and fibril formation *in vitro* [3], suppress Aβ accumulation and alleviate cognitive decline *in vivo* in Alzheimer's disease (AD) patients [4], lower amyloid deposition [5] and disrupt existing amyloid plaques in an AD transgenic mouse model [6].

Poorly soluble in water and typically soluble in solvents, the ability of curcumin (Fig. 1) to inhibit Aβ aggregation and fibril formation may possibly be related to its structural resemblance to Congo Red, a well-established amyloidophilic dye [4]. However, unlike Congo Red, curcumin is lipophilic and non-toxic. A majority of curcumin that is administered by oral and intra-peritoneal routes is confined to the gastrointestinal tract and undergoes metabolism to more polar and less potent derivatives such as the glucuronide and sulfate metabolites [7–12]. The poor systemic and plasma bioavailability of the active form of curcumin may pose a limitation on its usage as a potent therapeutic/nutraceutical agent to treat diseases outside the gastrointestinal tract. Its increased availability at the neurovascular junction of the cerebral microvasculature forming the blood brain barrier will be particularly desirable to treat neurological disorders such as AD and cerebrovascular amyloidosis.

In this study, we propose to load curcumin on to high-density lipoproteins (HDL), which are protein/lipid complexes that normally play a role in cholesterol transport in the plasma. Typically, plasma HDL may be spherical (~20 nm diameter) containing a core of neutral lipids like cholesteryl ester surrounded by amphipathic lipids such as phospholipids and cholesterol, and proteins such as apolipoproteins,

* Corresponding author. Department of Chemistry and Biochemistry, 1250 Bellflower Boulevard, California State University Long Beach, Long Beach, CA 90840, USA. Tel.: +1 562 985 4953; fax: +1 562 985 8557.
*E-mail address:* vnaraya2@csulb.edu (V. Narayanaswami).

0005-2736/$ – see front matter © 2010 Elsevier B.V. All rights reserved.
doi:10.1016/j.bbamem.2010.09.007

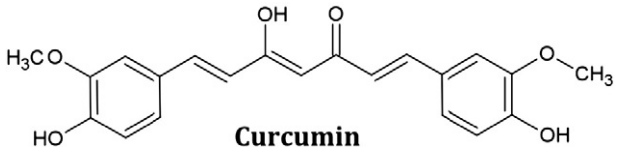


**Fig. 1.** Structure of curcumin. Curcumin (IUPAC name: 1,7-bis(4-hydroxy-3-methoxyphenyl)-1,6-heptadiene-3,5-dione) is the major curcuminoid of the spice turmeric. It has the capability of undergoing keto-enol tautomerization. The enol form (shown here) is more stable in solution under physiological conditions.

or discoidal (also recognized as nascent HDL) (5–20 nm diameter) composed of a bilayer of phospholipids (and cholesterol) surrounded by apolipoproteins [13]. Discoidal HDL can be reconstituted using apolipoprotein E3 (apoE3) or apolipoprotein AI (apoAI), another member of the apolipoprotein family, and are well-characterized in terms of their biophysical and biochemical characteristics [14]. They recapitulate the functional and structural features of native HDL isolated from the plasma. Importantly, the hydrophobic interior of the particle surrounded by the amphipathic helices of apolipoproteins offers an ideal environment to 'package' and transport curcumin in a predominantly aqueous environment such as the plasma.

Previous studies from our lab have derived structure–function relationships regarding apoE3 (reviewed in [14] and [15]), an anti-atherogenic protein that plays a critical role in regulating plasma and brain cholesterol homeostasis [16]. Considered an important protein in cardiovascular and Alzheimer's disease, apoE is an exchangeable apolipoprotein composed of an N-terminal (NT) domain (residues 1–191) and a C-terminal domain (201–299) linked by a protease-sensitive loop. The NT domain is a 4-helix bundle [14,17], which bears high-affinity binding sites for the cell-surface localized low density lipoprotein (LDL) receptor (LDLr) family of proteins [18]. Only lipid-associated apoE appears to bind to the LDLr; the binding leads to internalization and cellular uptake of the entire lipoprotein particle by receptor-mediated endocytosis. For LDLr binding to occur, the lipid-associated apoE may be in the form of very low density lipoproteins (VLDL) [19], native HDL [20] or reconstituted HDL containing synthetic phospholipids in the absence or presence of cholesterol [21]. In the present study, apoE-containing reconstituted HDL was deemed the flavonoid transporter of choice due to the ease of preparation of these particles, their well-characterized nature [15] and to the ability of these particles to interact with the LDLr. This will allow targeting of curcumin-loaded HDL to cells expressing LDLr. Our studies indicate that curcumin partitions efficiently into HDL as evidenced by fluorescence analysis, and that curcumin-bearing HDL prepared with apoE3-NT retains the structural integrity and a robust LDLr-binding activity comparable to those of HDL without curcumin.

## 2. Materials and methods

### 2.1. Chemicals

Potassium iodide (KI) and sodium thiosulfate were obtained from Fisher Scientific (Fair Lawn, NJ). Curcumin (98 + % pure) as a mixture of curcumin, demethoxycurcumin and bisdemethoxycurcumin was obtained from ACROS ORGANICS (Fair Lawn, NJ). 5 DOXYL-stearic acid, free radical (5-DSA) and 16 DOXYL-stearic acid, free radical (16-DSA) were purchased from Sigma-Aldrich (St. Louis, MO). Sephadex G-75 was from G.E. Healthcare (Uppsala, Sweden). Dimyristoylphosphatidylcholine (DMPC) was obtained from Avanti Polar Lipids (Alabaster, AL). The phospholipid assay kit was from Wako Chemicals USA, Inc. (Richmond, VA), the DC and the BCA kits for protein assay were from BioRad Laboratories (Hercules, CA) and Thermoscientific (Rockford, IL), respectively. All solvents used were of analytical grade.

### 2.2. Expression, isolation and purification of apoE3-NT

Recombinant human apoE3 residues 1–191 bearing a hexa-His tag at the N-terminal end was over-expressed in *E. coli*, isolated and purified using a Ni-affinity matrix (Hi-Trap chelating column, G.E. Healthcare, Uppsala, Sweden) as described earlier [22,23]. Protein purity was verified by SDS-PAGE analysis using a 4–20% acrylamide gradient.

#### 2.2.1. Reconstitution and characterization of HDL with curcumin

Reconstituted HDL containing dimyristoylphosphatidylcholine (DMPC) and apoE3-NT (5:2 w/w starting ratio) were prepared by the sonication method as described previously [24] and will be referred to as HDL throughout this study unless otherwise specified. HDL containing curcumin were prepared in a similar manner except that curcumin was included while making the DMPC thin film (Lipid:protein:curcumin ratio of 5:2:5 w/w). Lipid-free protein and curcumin not bound to HDL were separated from protein/lipid/curcumin ternary HDL complexes by gel filtration chromatography using Sephadex G-75 or by density gradient ultracentrifugation using KBr gradient. Fractions containing both protein and phospholipid were pooled based on absorbance at 280 nm and phospholipid assay, respectively. The presence of curcumin was determined by monitoring the absorbance of the individual fractions at 420 nm (molar extinction coefficient, 49,000 $M^{-1}$ $cm^{-1}$). Fractions containing co-localized protein, lipid and curcumin were pooled, concentrated and electrophoresced by agarose gel electrophoresis [25] using the TITAN GEL lipoprotein electrophoresis kit as described by the manufacturer (Helena Laboratories, Beaumont, TX). After electrophoresis the lipoproteins were transferred to a PVDF membrane by diffusion [26], the membranes probed with anti-apoE antibody mAb1D7 (Lipoproteins & Atherosclerosis Research Group, University of Ottawa Heart Institute, Ottawa, Ontario, Canada), and visualized by chemiluminescence using goat anti-mouse IgG-HRP (Millipore, Billerica, MA). HDL prepared in the absence or presence of curcumin was examined under a transmission electron microscope (Philips Electron Optics, Eindhoven, Netherlands) after negative staining with 1% phosphotungstate as described earlier [27].

### 2.3. Fluorescence spectroscopy

Steady state fluorescence analyses were performed on a Perkin-Elmer LS55B fluorometer at 24 °C. A stock solution of 5 mM curcumin was prepared in DMSO. Fluorescence emission spectra of curcumin were recorded in solvents of varying polarity and dielectric constant or in 10 mM sodium phosphate pH 7.4 containing 150 mM NaCl (phosphate-buffered saline or PBS) or in PBS containing 0.1% TX-100. The samples were excited at 420 nm and the emission spectra were recorded between 450 and 650 nm. The excitation and emission slit-widths were set at 5 nm and the scan speed at 50 nm/min; typically 3 scans were averaged.

### 2.4. Quenching studies

To verify the location of curcumin in the HDL, the fluorescence emission of curcumin was quenched with KI and spin-labeled fatty acids (5-DSA and 16-DSA) as described earlier [28]. Briefly, fluorescence quenching studies were performed by addition of small increments of stock solutions of KI in buffer or 5-DSA or 16-DSA (stock solutions in DMSO) directly to 400 μl of HDL with curcumin in PBS (50 μg protein). In experiments where DMSO was used, the final concentration of the solvent was always ≤5% v/v. The KI stock solutions contained 1 mM sodium thiosulfate to prevent formation of free iodine. The fluorescence emission intensities were recorded at 495 nm in the absence and presence of varying amounts of quenchers. The apparent Stern–Volmer quenching constants ($K_{SV}$) were calculated employing the Stern–Volmer equation, $F_0/F = 1 + K_{SV}[Q]$, where $F_0$ and F

are fluorescence intensities in the absence and presence of varying quencher concentrations, respectively, and [Q] is the quencher concentration [29–31].

### 2.5. Dose-dependent loading of curcumin into HDL

To determine the amount of curcumin that can be loaded on to a pre-existing HDL particle, 10 μg HDL protein was treated with increasing concentrations of curcumin in DMSO, and incubated at 37 °C for 6 h. Fluorescence emission spectra of the samples were recorded and the fluorescence emission intensity at 495 nm plotted versus curcumin concentration. The size of the particles in the absence or presence of varying amounts of curcumin was determined by non-denaturing polyacrylamide gel electrophoresis (PAGE) on a 4–20% acrylamide gradient. Following gel electrophoresis, the lipoproteins were visualized using Amido Black stain.

### 2.6. LDLr binding assay

To assess whether curcumin loading affected the LDLr binding activity of HDL with apoE3-NT, we performed an a co–immunoprecipitation (co–IP) analysis, as described earlier [32,33]. A construct bearing the LDLr ligand binding domains 3–6 with a c-Myc epitope was employed. This construct represents the essential ligand binding elements of the extra cellular soluble portion of the mature LDLr and will be represented as sLDLr unless otherwise specified. HDL (5 μg apoE3-NT protein) prepared with or without curcumin was incubated with 5 μg of sLDLr in the presence of $Ca^{2+}$ for 16 h at 4 °C, followed by IP using anti-c-Myc-Agarose (Sigma-Aldrich, St. Louis, MO). sLDLr-bound apoE was detected by Western blot using HRP-conjugated polyclonal apoE antibody. In control reactions, the HDL was omitted in the incubation mixture.

## 3. Results and discussion

A characteristic feature of apolipoproteins is their ability to transform phospholipid vesicles to discoidal bilayer protein–lipid complexes. The protein–lipid complexes resemble nascent pre-β HDL [34,35] generated *in vivo*; they are composed of a bilayer of phospholipids that are encircled by a series of amphipathic α-helices of the apolipoproteins, which prevent exposure of the hydrophobic fatty acyl chains of the phospholipids to the aqueous environment. In this arrangement, the helical axes of the protein are oriented perpendicular to the fatty acyl chains of the phospholipids [36,37]; the hydrophobic face of the helices is oriented towards the fatty acyl chains and the polar side chains face the aqueous environment. In the present study, we take advantage of the presence of the hydrophobic milieu of the lipid interior of the HDL particle as a discrete environment to package the highly hydrophobic curcumin molecules. The presence of the receptor-binding sites on helix 4 of apoE3-NT [17] is a desirable feature since it facilitates 'homing' and lipoprotein receptor binding.

HDL with (Fig. 2A) or without (Fig. 2B) curcumin was applied to a gel filtration column at a flow rate of 1 ml/min and the fractions were monitored at 280 and 420 nm for the presence of protein and curcumin, respectively. The presence of apoE3-NT in individual fractions was also visualized by SDS-PAGE (insets in Fig. 2A and B). It must be pointed out that curcumin displays significant absorbance at 280 nm, which likely accounts for the high absorbance noted for fractions containing HDL with curcumin (Fig. 2A). The phospholipid content in each fraction was determined to verify the presence of lipids (data not shown). In separate experiments, HDL prepared with or without curcumin was also isolated by density gradient ultracentrifugation. Fig. 3 shows the image of the tube containing HDL and curcumin prior to fractionation. Each fraction was analyzed for the presence of protein, lipid and curcumin and the protein visualized by SDS-PAGE analysis. As indicated by the arrow in the figure, curcumin co-localizes with fractions containing protein and lipid, at densities corresponding to those of HDL in a KBr gradient (1.063–1.21 g/ml) [25]. In both isolation protocols, fractions containing co-localized

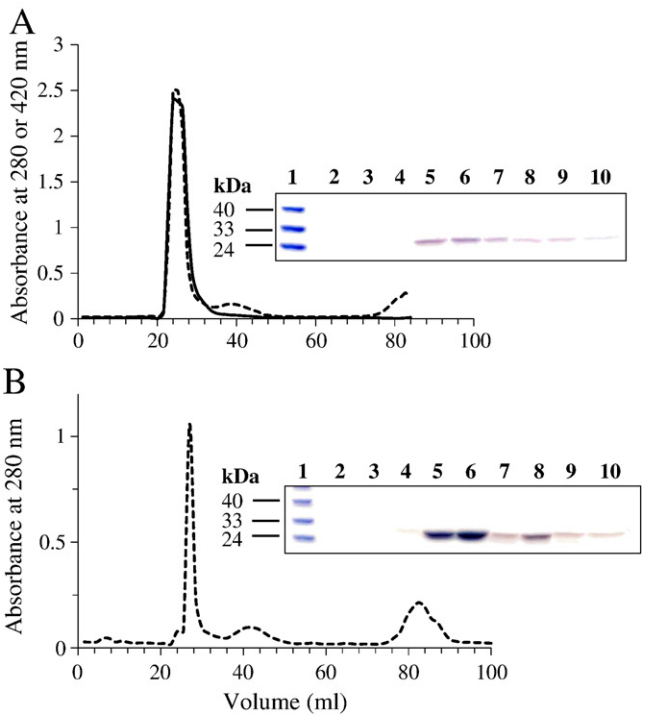


**Fig. 2.** Isolation of HDL containing curcumin by gel filtration chromatography. HDL with (panel A) or without (panel B) curcumin was applied to a Sephadex G-75 gel filtration column at a flow rate of 1 ml/min in PBS. The fractions were analyzed for the presence of protein (dotted line) and curcumin (bold line) by monitoring the absorbance at 280 and 420 nm, respectively. Inset. SDS-PAGE analysis of individual fractions was performed to visualize the presence of apoE3-NT. Lane 1 in both gels represents the low molecular weight standard with the indicated molecular masses. In panel A, lanes 2 to 10 represent elution volumes in 1.2 ml increments between 20.4 and 30 ml, while in panel B lanes 2 to 10 represent elution volumes in 1.5 ml increments between 21 and 33 ml.

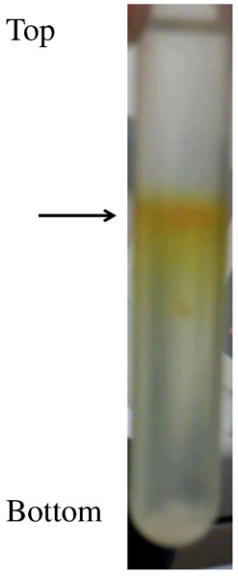


**Fig. 3.** Density gradient ultracentrifugation of HDL with curcumin. HDL containing curcumin was separated from lipid-free protein and curcumin not bound to HDL by density gradient ultracentrifugation as described previously [24]. The image shows co-localization of curcumin with lipoprotein complexes (arrow) that migrate to densities corresponding to that of HDL in a KBr gradient.

protein, lipid and curcumin were pooled. In control experiments, HDL without curcumin was isolated in an identical manner. All data reported in this study were obtained with HDL isolated by the gel filtration method; similar results were obtained (data not shown) when HDL was isolated by density gradient ultracentrifugation approach.

Agarose gel electrophoresis and electron microscopic analysis of HDL in the presence and absence of curcumin were carried out (Fig. 4). The agarose gel was stained for lipid (data not shown as the lipid stains used have a low affinity for phospholipids) and independently evaluated for protein by Western blot analysis (Fig. 4A). Immunoblot of the agarose gel revealed that the electrophoretic mobility of apoE3-NT containing HDL particles with curcumin is similar to that of apoE3-NT HDL without curcumin and that they migrate with similar mobility to zones intermediate between the alpha and beta positions as described by Sparks & Phillips for apoAI [25]. Electron microscopy of the lipoprotein complexes in the presence of curcumin (Fig. 4B), revealed the formation of HDL-like particles with an average diameter of 25.1 ± 0.2nm (n = 87) seen as both stacked and en face discoidal structures. The geometry and size were comparable to those of HDL without curcumin (Fig. 4C), with average diameters of 23.7 ± 0.1 nm (n = 176). Panel B has fewer discoidal particles as the sample was dilute. Both panels display sample heterogeneity, consistent with the observations from lipogel analysis. These studies confirm that the presence of curcumin does not significantly alter the structural integrity, geometry or size of the HDL particle [24]. Particle composition analysis reveals that the lipid to protein ratio of HDL with curcumin is about 70:1 (M/M) and curcumin:protein ratio of about 8:1.

We took advantage of the intrinsic fluorescence of curcumin to determine if curcumin is present within the HDL particle or if it simply co-migrated with the HDL loosely bound to the external surface of the particle. In the former case, the environment of the curcumin molecules in the phospholipid bilayer within the head group region can be expected to be hydrophobic; however, in the latter case it can be expected to be polar, which is reflective of the nature of the aqueous environment surrounding the HDL particle. To address this issue, in initial experiments, fluorescence emission analysis of curcumin (~0.1 μg/ml) was carried out in solvents of varying polarity, such as methanol (a), ethanol (b), tetrahydrofuran (c) and ethyl acetate (d) (dielectric constants of 33.0, 24.3, 7.5 and 6.0, respectively) to obtain a correlation between the microenvironment polarity and fluorescence emission characteristics of curcumin (Fig. 5, panel A).

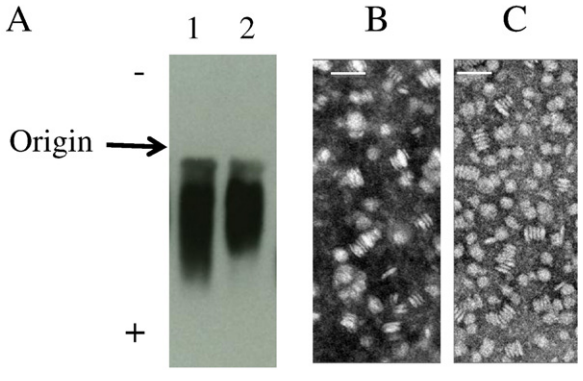


**Fig. 4.** Agarose gel electrophoresis and electron micrographs of HDL without and with curcumin. Lipoprotein gel electrophoresis of HDL (1 μg apoE3-NT) (panel A) was performed in an agarose gel. The electrophoresis was carried out at 80 V for 45 min followed by diffusion transfer of proteins to PVDF membrane and Western blot analysis using anti-apoE antibody (mAb1D7). Lane 1: HDL with curcumin; lane 2: HDL without curcumin. Electron microscopic analysis of HDL with (panel B) or without curcumin (panel C) was carried out following negative staining of the particles with 1% phosphotungstate. The bar represents 50 nm.

Curcumin was soluble in these solvents (more readily soluble in tetrahydrofuran and ethyl acetate). The wavelength of maximal fluorescence emission intensity ($\lambda_{max}$) was ~570 nm in methanol, ~559 nm in ethanol, ~518 nm in tetrahydrofuran and ~514 nm in ethyl acetate. It is noted that as the solvent polarity decreases, there is a corresponding decrease in the $\lambda_{max}$. This blue shift is accompanied by a general increase in the fluorescence emission intensity, a behavior predicted to occur with fluorophores present in a less polar solvent [39]. In contrast, curcumin displays little or no fluorescence emission in aqueous buffers such as PBS (in which it is poorly soluble) (Fig. 5, panel B, *spectrum a*). In the presence of detergent micelles such as 0.1% TX-100 (*spectrum b*), curcumin displays intense fluorescence emission with a $\lambda_{max}$ at 493 nm. The increased intensity and blue-shifted spectrum are indicative of interaction of curcumin with the detergent micelles and relocation to the hydrophobic interior of the micellar structure. Interestingly, curcumin that has co-migrated with the HDL fraction displays a $\lambda_{max}$ of ~495 nm, with a shoulder ~470 nm (*spectrum c*). From this observation, we infer that curcumin has relocated into the hydrophobic environment in the interior of the phospholipid bilayer of the HDL. The shoulder may represent the presence of a second population of curcumin in a discrete microenvironment within a single particle in addition to those in the hydrophobic milieu; one such site is at the protein–lipid interface of the HDL where the non-polar surface of the amphipathic helices around the particle perimeter face the fatty acyl chains of the phospholipid bilayer. Alternatively, the shoulder may be due to the presence of subpopulations of HDL (as noted in Fig. 4 by agarose gel electrophoresis, in Fig. 5 by non-denaturing PAGE) into which curcumin was distributed. Lastly, the possibility that the spectrum represents the two tautomeric forms of curcumin cannot be excluded at this point, as it is believed that curcumin can undergo keto-enol tautomerization under physiological conditions [2].

To determine if HDL loading of curcumin is saturable, increasing amounts of curcumin (5 mM stock dissolved in DMSO) was incubated with HDL (10 μg protein) at 37 °C for 6 h. Fluorescence emission spectra of the incubation mixtures revealed a gradual increase in fluorescence emission intensity with increasing curcumin concentration. Fig. 5, panel C shows a plot of fluorescence emission intensity at 495 nm versus concentration of added curcumin. The curve is reflective of a steady increase in localization of curcumin in a lipophilic environment followed by a plateau around 50 μM curcumin, indicative of saturable binding. Non-denaturing PAGE of HDL that was incubated with 0, 50 or 500 μg curcumin (added directly to 50 μg HDL protein) revealed the presence of protein/lipid complexes with an apparent molecular mass of ~670 kDa (Fig. 5, panel D). This corresponds to a particle diameter of ~17 nm based on the Stokes' diameter of the standards (note that the diameter obtained from the electron micrographs was ~25 nm). The differences noted in the particle diameters obtained from two different methods are attributed to the limitations inherent with each method. Typically, the diameters of lipoprotein particles obtained from electron microscopy measurements are significantly higher than those from other methods such as non–denaturing PAGE [40,41]. While neither approaches yield accurate information regarding particle diameter, we believe that the diameter of the reconstituted HDL bearing curcumin is in the range generally observed for apoE-containing particles prepared in similar ways [24,42]. Previously, we suggested that there may be 4–6 apoE3-NT/discoidal particle based on particle composition and size [38]. Employing similar calculations, we estimate that under the current preparation conditions wherein curcumin is added during the reconstitution procedure, each HDL particle has 30–50 curcumin molecules. However, from the dose-dependent fluorescence analysis, it appears that the HDL particle may be able to accommodate at least three times more curcumin. Further studies are needed to verify this possibility and to understand the loading capacity and stability of a loaded HDL particle.

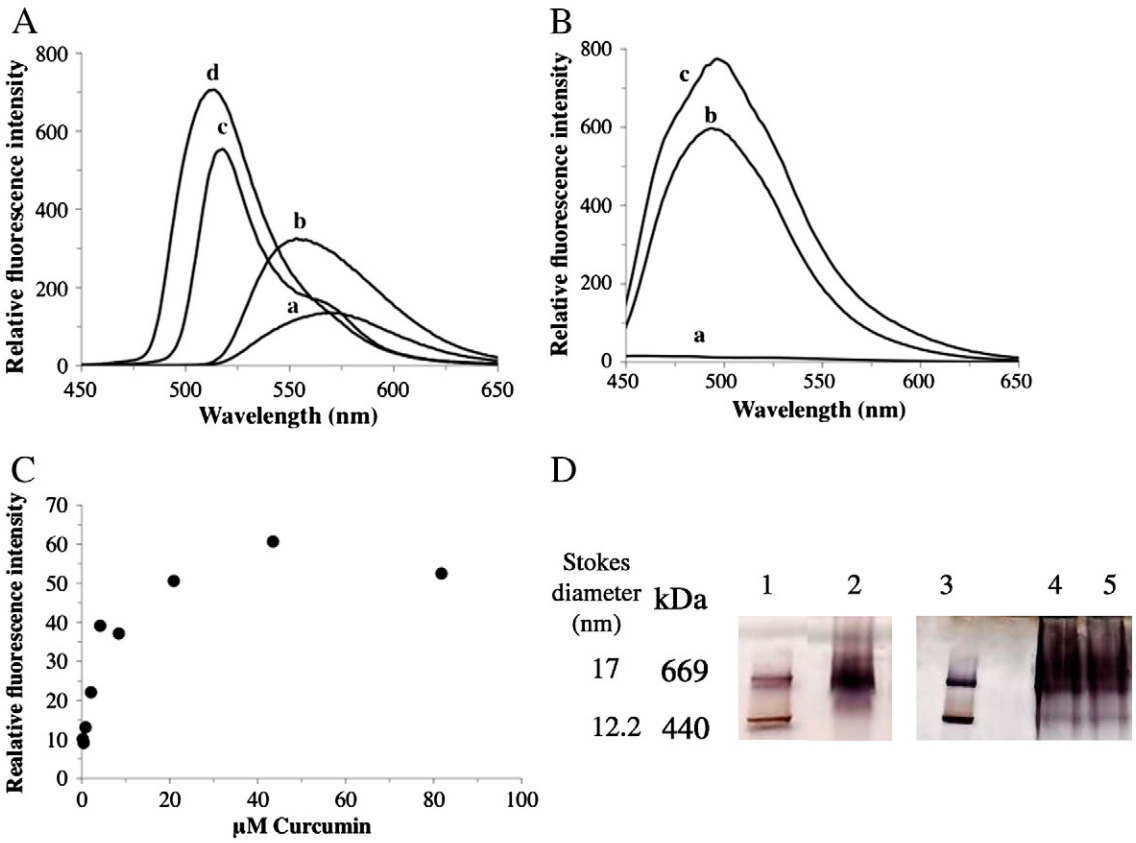


**Fig. 5.** Fluorescence emission spectra of curcumin. Panel A shows fluorescence emission spectra of curcumin in solvents of varying polarity such as methanol (a), ethanol (b), tetrahydrofuran (c) and ethyl acetate (d) with dielectric constants of 33.0, 24.3, 7.5 and 6.0, respectively. The spectra were recorded between 450 and 650 nm following excitation at 420 nm. Panel B shows fluorescence emission spectra of curcumin in PBS (a), 0.1% TX-100 (b) or reconstituted HDL (15 μg protein) (c). Panel C shows the dose-dependent accumulation of curcumin in HDL. Curcumin (5 mM stock dissolved in DMSO) was added in incremental amounts to HDL (10 μg apoE protein) and incubated at 37 °C for 6 h. The fluorescence emission intensities at 495 nm were plotted versus the final curcumin concentration in the incubation mixture. A representative plot from 3 different experiments is shown. Panel D. Non-denaturing PAGE of HDL in the presence of varying amounts of curcumin. HDL was incubated with 0, 50 and 500 μg curcumin (added to 50 μg HDL protein) as described above, electrophoresced on 4–20% acrylamide gradients (lanes 2, 4 and 5, respectively) and stained with Amido Black. Lanes 1 and 3 show high molecular weight standards, thyroglobulin (669 kDa) and ferritin (440 kDa) bearing Stokes' diameter of 17 and 12.2 nm, respectively.

To verify the location of curcumin with respect to the HDL, the fluorescence emission of curcumin was quenched using quenchers that are known to be water-soluble (KI) or lipid-soluble (5-DSA and 16-DSA). The rationale behind this analysis is that KI represents a class of aqueous, dynamic quenchers that involve collision between a fluorophore and a heavy atom (such as iodide ion in this case); thus, if curcumin is located on the periphery of the HDL facing the aqueous environment, its fluorescence will be quenched readily by KI. On the other hand, fatty acids are lipophilic molecules that partition rapidly into the phospholipid bilayer; the DOXYL spin labels present on the fatty acid are excellent quenchers of fluorescence emission. If curcumin is present in the hydrophobic milieu of the phospholipid bilayer of the HDL, its fluorescence will be quenched efficiently by the DOXYL group on the fatty acid. Fatty acids are expected to insert into the lipid bilayer with the hydrophobic tail facing inward and the carboxylic acid facing the aqueous environment. Further by comparing the quenching constants using 5-DSA and 16-DSA, we can estimate the depth of location of curcumin in the preparations since the DOXYL group (on C16 position) in 16-DSA will be located deeper than that in 5-DSA. Fig. 6A and C show plots of $F/F_0$ versus quencher concentration for quenching of curcumin fluorescence by increasing concentrations of KI and DOXYL-stearic acids, respectively. Both DOXYL-stearic acids were far more powerful quenching agents compared to KI, displaying apparent Stern–Volmer quenching constants of $7.37 \pm 1.71 \times 10^{-3}$ $M^{-1}$ for 16-DSA and $2.45 \pm 0.43 \times 10^{-3}$ $M^{-1}$ for 5-DSA (Fig. 6D) versus $0.23 \pm 0.04$ $M^{-1}$ for KI (Fig. 6B). An interesting observation that emerged upon comparison of the quenching curves of the two DOXYL-stearic acids is that the $K_{SV}$ for 16-DSA is about 3-fold higher than that for 5-DSA. From these observations, we propose that curcumin is located deep within the lipid bilayer in the HDL, an inference that derives further supporting evidence from the highly blue-shifted fluorescence emission spectrum of curcumin (Fig. 5B, *spectrum c*).

Lastly, an LDLr binding assay was performed by IP analysis as described previously [32,33] to determine if curcumin-loaded HDL retains its functional ability. HDL (5 μg apoE3-NT protein) prepared with or without curcumin was incubated with sLDLr in the presence of $Ca^{2+}$ for 16 h at 4 °C. The sLDLr/HDL complex was captured by incubation with anti-c-Myc-Agarose, followed by Western blot analysis to detect apoE, Fig. 7. The presence of a band corresponding to the 22-kDa apoE3-NT indicates an ability of HDL to interact with sLDLr. HDL with curcumin (lane 2) displays a robust binding with sLDLr, similar to that displayed by HDL without curcumin (lane 1). In control incubations, apoE-bearing HDL was omitted; these samples did not show sLDLr binding (lane 3). Lanes 4 and 5 are Western blot controls containing reconstituted HDL with apoE (1 μg protein) in the absence and presence of curcumin, respectively. The binding interaction between the LDLr and apoE3-NT involves participation of

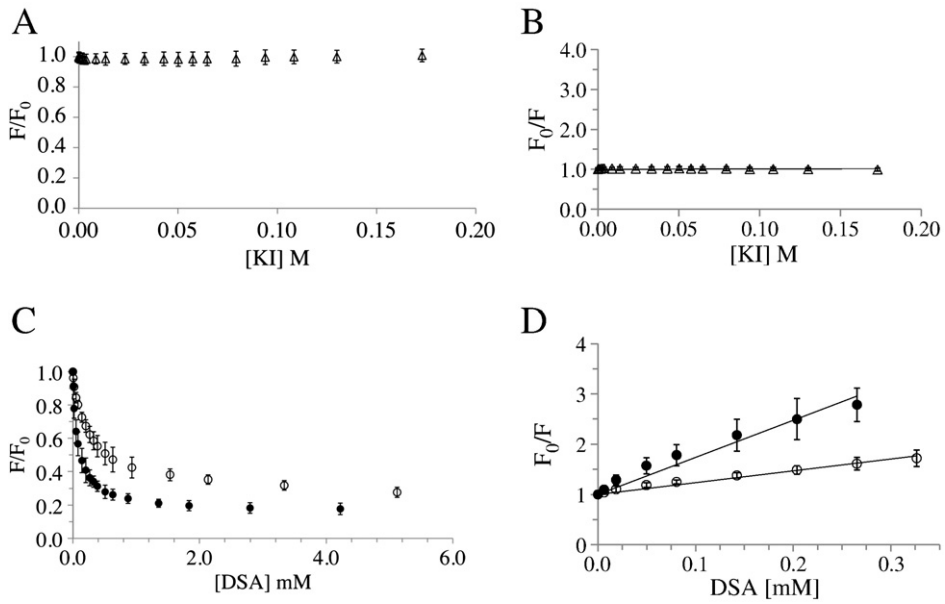


**Fig. 6.** Quenching analysis of HDL with curcumin. HDL with curcumin (10 μg protein) was treated with increasing concentrations of KI in PBS (panels A and B) or DOXYL-stearic acid in DMSO (panels C and D), and the fluorescence emission intensity recorded at each concentration at 495 nm (excitation at 420 nm). KI, open triangles; 5-DSA, open circles, and 16-DSA, closed circles. The data are plotted as $F/F_0$ versus quencher concentration (panels A and C), or as the Stern–Volmer plot of $F_0/F$ versus quencher concentration (panels B and D). The Stern–Volmer quenching constants were obtained from the slopes of the line fitted to the equation as described under Materials and methods. Data are represented as mean ± SD from 3 or 4 independent experiments.

several sites on the ligand (and the receptor), with multiple apoE molecules on the HDL involved in co-operative binding. Our results suggest that the presence of curcumin does not alter the ability of HDL-bound apoE3 to interact with the LDLr. This feature can be exploited in future studies to facilitate cellular uptake and internalization of the curcumin-loaded HDL with apoE by receptor-mediated endocytosis. Any cell type having the LDLr (or the family of receptors for many of which apoE is a ligand) may benefit from this mode of delivery. It is noteworthy that the brain microvasculature endothelial cells have significantly higher expression of LDLr on the side facing the vasculature [43] compared to the peripheral arterial endothelial cells. This is because the latter lacks a constitutively functional LDLr due to contact inhibition (being in constant contact with the physiological concentration of LDL, there is a down-regulation of the LDLr expression [43]). Thus, HDL bearing apoE may prove to be advantageous to make curcumin more bioavailable at the neurovascular junction lining the blood brain barrier.

In previous studies from other labs, similar protein–lipid complexes formed as a result of self-assembly under appropriate conditions, have been called nanodiscs since they are discoidal in shape bearing diameters that are in the nanometer scale (~10 nm or lower). They are soluble in aqueous environments and have been used to study membrane proteins [44–46] or to 'package' select small molecules of pharmaceutical interest [47] with truncated apoAI as the membrane scaffold protein that surrounds a bilayer containing dipalmitoylphosphatidylcholine or palmitoyloleoylphosphatidylcholine. In our study, we employed discoidal particles containing apoE, which, unlike apoAI, has the ability to bind to the LDLr, for transport of curcumin in plasma and targeted delivery to cell surfaces expressing the receptor family of proteins. These HDL-like complexes bearing apoE are well-characterized [24,37,38,48], soluble, stable, and provide a discrete hydrophobic environment to transport curcumin, protecting it from rapid metabolism to less potent forms. Researchers have been able to manipulate the size of the nanodiscs [45] by varying the length of apoAI; the lipid: protein molar ratio varied (ranging from 75:1 to 200:1) depending on the nature of the lipid and the apoAI construct. Under the conditions described in our case, we obtained larger discoidal particles with a ratio of 70:1. The difference may be attributed to the use of apoE, higher copy numbers of apoE/particle, and/or the presence of about 30–50 molecules of curcumin per particle in our preparations. More studies are needed to determine if the loading capacity is related to the lipid composition of the HDL.

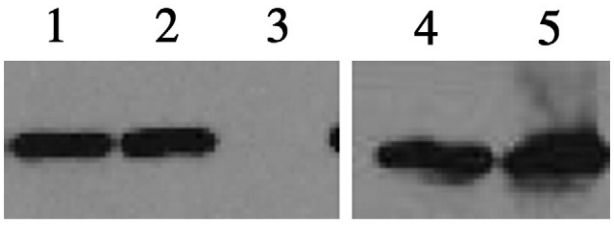


**Fig. 7.** Effect of curcumin on sLDLr binding of HDL. HDL without or with curcumin (5 μg protein) were incubated with 5 μg of sLDLr in 25 mM Tris–HCl, pH 7.4, 140 mM NaCl, 27 mM KCl, 2 mM $CaCl_2$ for 16 h at 4 °C, followed by IP with anti-c-Myc-Agarose. sLDLr-bound apoE was detected by Western blot using HRP-conjugated polyclonal apoE antibody. The lane assignments are as follows: lane 1, HDL with no curcumin; lane 2, HDL with curcumin; lane 3, no HDL. Lanes 4 and 5 represent Western blot controls containing HDL (1 μg) without and with curcumin, respectively.

ApoE-containing HDL particles are of direct relevance for curcumin transport since apoE appears to be the primary apolipoprotein in the CNS where it is located on HDL-sized particles [20,49,50]; no large lipoprotein particles have been identified in the CNS. There appears to be no major exchange of apoE and cholesterol between the vascular system and CNS [51,52]. ApoE is one of the best known genetic risk factors for AD with individuals homozygous for the *APOE* ε4 allele having a 50–90% chance of developing AD by 85 years of age, while heterozygous subjects have a chance of 45%. The amino acid at position 112 differs in the two major isoforms, apoE3 and apoE4: it is Cys in apoE3 and Arg in apoE4. The molecular basis for the difference in their physiological and pathological behavior in AD is not fully understood, and may involve a combination of factors [15].

Other groups have shown binding and/or stabilization of curcumin following a direct binding interaction with serum albumin and fibrinogen [53–55]. Although these proteins represent a bulk of the plasma proteins, HDL with apoE can serve as a versatile 'nanovehicle' to transport curcumin by providing a sheltered hydrophobic

microenvironment to decrease its degradation and therefore increase its bioavailability, and to target curcumin due to the ability of apoE to serve as a ligand for the LDLr. Additionally, it may serve as a potent lipid-based antioxidant to protect LDL from oxidation, an aspect investigated by some researchers studying partitioning of similar ferulic acid derivatives into plasma lipoprotein fractions [56]. The curcumin used in our study contains small amounts (2%) of demethoxycurcumin and bisdemethoxycurcumin, both reported to possess anti-inflammatory and antioxidant properties. However, their potencies relative to curcumin appear to be widely variable depending on the system and the experimental conditions used, with reports of similar potencies [57], lower potency [58,59], or higher potency for the derivatives compared to that of curcumin [60].

### 3.1. Concluding remarks

In conclusion, use of reconstituted HDL bearing the apoE3 receptor-binding domain shows promise of increasing the bioavailability of curcumin, and potentially other lipophilic agents, to possibly treat inflammation, oxidative stress and complex neurological diseases such as AD and cerebrovascular amyloidosis.

## Acknowledgements

This work was funded by the Tobacco Related Disease Research Program (TRDRP 17RT-0165), NIH-HL096365, the Drake Family Trust (VN), CSULB & Women & Philanthropy Award (PK). We thank Malathi Kosaraju, Children's Hospital Oakland Research Institute, for help with the agarose gel electrophoresis, and Don Gantz and Drs. Shobini Jayaraman and Olga Gursky, Boston University School of Medicine, Boston, MA for the EM analysis and helpful discussions.

## References

[1] G.J. Kelloff, C.W. Boone, J.A. Crowell, V.E. Steele, R.A. Lubet, L.A. Doody, W.F. Malone, E.T. Hawk, C.C. Sigman, New agents for cancer chemoprevention, J. Cell. Biochem. Suppl. 26 (1996) 1–28.
[2] R.A. Sharma, A.J. Gescher, W.P. Steward, Curcumin: the story so far, Eur. J. Cancer. 41 (2005) 1955–1968.
[3] K. Ono, K. Hasegawa, H. Naiki, M. Yamada, Curcumin has potent anti-amyloidogenic effects for Alzheimer's beta-amyloid fibrils in vitro, J. Neurosci. Res. 75 (2004) 742–750.
[4] F. Yang, G.P. Lim, A.N. Begum, O.J. Ubeda, M.R. Simmons, S.S. Ambegaokar, P.P. Chen, R. Kayed, C.G. Glabe, S.A. Frautschy, G.M. Cole, Curcumin inhibits formation of amyloid beta oligomers and fibrils, binds plaques, and reduces amyloid in vivo, J. Biol. Chem. 280 (2005) 5892–5901.
[5] G.P. Lim, T. Chu, F. Yang, W. Beech, S.A. Frautschy, G.M. Cole, The curry spice curcumin reduces oxidative damage and amyloid pathology in an Alzheimer transgenic mouse, J. Neurosci. 21 (2001) 8370–8377.
[6] M. Garcia-Alloza, L.A. Borrelli, A. Rozkalne, B.T. Hyman, B.J. Bacskai, Curcumin labels amyloid pathology in vivo, disrupts existing plaques, and partially restores distorted neurites in an Alzheimer mouse model, J. Neurochem. 102 (2007) 1095–1104.
[7] B. Wahlstrom, G. Blennow, A study on the fate of curcumin in the rat, Acta Pharmacol. Toxicol. (Copenh) 43 (1978) 86–92.
[8] V. Ravindranath, N. Chandrasekhara, Metabolism of curcumin—studies with [3H] curcumin, Toxicology 22 (1981) 337–344.
[9] M.H. Pan, T.M. Huang, J.K. Lin, Biotransformation of curcumin through reduction and glucuronidation in mice, Drug Metab. Dispos. 27 (1999) 486–494.
[10] C. Ireson, S. Orr, D.J. Jones, R. Verschoyle, C.K. Lim, J.L. Luo, L. Howells, S. Plummer, R. Jukes, M. Williams, W.P. Steward, A. Gescher, Characterization of metabolites of the chemopreventive agent curcumin in human and rat hepatocytes and in the rat in vivo, and evaluation of their ability to inhibit phorbol ester-induced prostaglandin E2 production, Cancer Res. 61 (2001) 1058–1064.
[11] C.R. Ireson, D.J. Jones, S. Orr, M.W. Coughtrie, D.J. Boocock, M.L. Williams, P.B. Farmer, W.P. Steward, A.J. Gescher, Metabolism of the cancer chemopreventive agent curcumin in human and rat intestine, Cancer Epidemiol. Biomarkers. Prev. 11 (2002) 105–111.
[12] R.A. Sharma, C.R. Ireson, R.D. Verschoyle, K.A. Hill, M.L. Williams, C. Leuratti, M.M. Manson, L.J. Marnett, W.P. Steward, A. Gescher, Effects of dietary curcumin on glutathione S-transferase and malondialdehyde-DNA adducts in rat liver and colon mucosa: relationship with drug levels, Clin. Cancer Res. 7 (2001) 1452–1458.
[13] S. Lund-Katz, M.C. Phillips, High density lipoprotein structure–function and role in reverse cholesterol transport, Subcell. Biochem. 51 (2010) 183–227.
[14] V. Narayanaswami, R.S. Kiss, P.M. Weers, The helix bundle: a reversible lipid binding motif, Comp. Biochem. Physiol. A. Mol. Integr. Physiol. 155 (2010) 123–133.
[15] E.P. de Chaves, V. Narayanaswami, Apolipoprotein E and cholesterol in aging and disease in the brain, Future Lipidol. 3 (2008) 505–530.
[16] R.W. Mahley, Y. Huang, K.H. Weisgraber, Putting cholesterol in its place: apoE and reverse cholesterol transport, J. Clin. Invest. 116 (2006) 1226–1229.
[17] C. Wilson, M.R. Wardell, K.H. Weisgraber, R.W. Mahley, D.A. Agard, Three-dimensional structure of the LDL receptor-binding domain of human apolipoprotein E, Science 252 (1991) 1817–1822.
[18] K.H. Weisgraber, Apolipoprotein E: structure–function relationships, Adv. Protein Chem. 45 (1994) 249–302.
[19] C.D. Mamotte, M. Sturm, J.I. Foo, F.M. van Bockxmeer, R.R. Taylor, Comparison of the LDL-receptor binding of VLDL and LDL from apoE4 and apoE3 homozygotes, Am. J. Physiol. 276 (1999) E553–E557.
[20] R.E. Pitas, J.K. Boyles, S.H. Lee, D. Foss, R.W. Mahley, Astrocytes synthesize apolipoprotein E and metabolize apolipoprotein E-containing lipoproteins, Biochim. Biophys. Acta. 917 (1987) 148–161.
[21] A. Lalazar, K.H. Weisgraber, S.C. Rall Jr., H. Giladi, T.L. Innerarity, A.Z. Levanon, J.K. Boyles, B. Amit, M. Gorecki, R.W. Mahley, et al., Site-specific mutagenesis of human apolipoprotein E. Receptor binding activity of variants with single amino acid substitutions, J. Biol. Chem. 263 (1988) 3542–3545.
[22] V. Gupta, V. Narayanaswami, M.S. Budamagunta, T. Yamamato, J.C. Voss, R.O. Ryan, Lipid-induced extension of apolipoprotein E helix 4 correlates with low density lipoprotein receptor binding ability, J. Biol. Chem. 281 (2006) 39294–39299.
[23] N. Choy, V. Raussens, V. Narayanaswami, Inter-molecular coiled-coil formation in human apolipoprotein E C-terminal domain, J. Mol. Biol. 334 (2003) 527–539.
[24] V. Narayanaswami, J.N. Maiorano, P. Dhanasekaran, R.O. Ryan, M.C. Phillips, S. Lund-Katz, W.S. Davidson, Helix orientation of the functional domains in apolipoprotein e in discoidal high density lipoprotein particles, J. Biol. Chem. 279 (2004) 14273–14279.
[25] D.L. Sparks, M.C. Phillips, Quantitative measurement of lipoprotein surface charge by agarose gel electrophoresis, J. Lipid. Res. 33 (1992) 123–130.
[26] T.M. Forte, J.K. Bielicki, R. Goth-Goldstein, J. Selmek, M.R. McCall, Recruitment of cell phospholipids and cholesterol by apolipoproteins A-II and A-I: formation of nascent apolipoprotein-specific HDL that differ in size, phospholipid composition, and reactivity with LCAT, J. Lipid Res. 36 (1995) 148–157.
[27] O. Gursky, Ranjana, D.L. Gantz, Complex of human apolipoprotein C-1 with phospholipid: thermodynamic or kinetic stability? Biochemistry 41 (2002) 7373–7384.
[28] S. Tamamizu-Kato, M.G. Kosaraju, H. Kato, V. Raussens, J.M. Ruysschaert, V. Narayanaswami, Calcium-triggered membrane interaction of the alpha-synuclein acidic tail, Biochemistry 45 (2006) 10947–10956.
[29] J.R. Lakowicz, Quenching of Fluorescence, and Advanced Topics in Fluorescence Quenching. Principles of Fluorescence Spectroscopy, Kluwer Academic/Plenum, New York, 1999 pp. 238–289.
[30] D. Sahoo, V. Narayanaswami, C.M. Kay, R.O. Ryan, Pyrene excimer fluorescence: a spatially sensitive probe to monitor lipid-induced helical rearrangement of apolipophorin III, Biochemistry 39 (2000) 6594–6601.
[31] M.R. Eftink, C.A. Ghiron, Exposure of tryptophanyl residues in proteins, Quantitative determination by fluorescence quenching studies, Biochemistry 15 (1976) 672–680.
[32] S. Tamamizu-Kato, J.Y. Wong, V. Jairam, K. Uchida, V. Raussens, H. Kato, J.M. Ruysschaert, V. Narayanaswami, Modification by acrolein, a component of tobacco smoke and age-related oxidative stress, mediates functional impairment of human apolipoprotein E, Biochemistry 46 (2007) 8392–8400.
[33] C. Fisher, D. Abdul-Aziz, S.C. Blacklow, A two-module region of the low-density lipoprotein receptor sufficient for formation of complexes with apolipoprotein E ligands, Biochemistry 43 (2004) 1037–1044.
[34] S.T. Kunitake, K.J. La Sala, J.P. Kane, Apolipoprotein A-I-containing lipoproteins with pre-beta electrophoretic mobility, J. Lipid. Res. 26 (1985) 549–555.
[35] B.Y. Ishida, J. Frolich, C.J. Fielding, Prebeta-migrating high density lipoprotein: quantitation in normal and hyperlipidemic plasma by solid phase radioimmunoassay following electrophoretic transfer, J. Lipid. Res. 28 (1987) 778–786.
[36] V. Raussens, V. Narayanaswami, E. Goormaghtigh, R.O. Ryan, J.M. Ruysschaert, Alignment of the apolipophorin-III alpha-helices in complex with dimyristoyl-phosphatidylcholine. A unique spatial orientation, J. Biol. Chem. 270 (1995) 12542–12547.
[37] J. Drury, V. Narayanaswami, Examination of lipid-bound conformation of apolipoprotein E4 by pyrene excimer fluorescence, J. Biol. Chem. 280 (2005) 14605–14610.
[38] C.A. Fisher, V. Narayanaswami, R.O. Ryan, The lipid-associated conformation of the low density lipoprotein receptor binding domain of human apolipoprotein E, J. Biol. Chem. 275 (2000) 33601–33606.
[39] J.R. Lakowicz, Protein Fluorescence, Kluwer Academic / Plenum Publishers, New York, Principles of Fluorescence Spectroscopy, 1999 pp. 445–486.
[40] J.H. Wald, E. Coormaghtigh, J. De Meutter, J.M. Ruysschaert, A. Jonas, Investigation of the lipid domains and apolipoprotein orientation in reconstituted high density lipoproteins by fluorescence and IR methods, J. Biol. Chem. 265 (1990) 20044–20050.
[41] A.V. Nichols, E.L. Gong, P.J. Blanche, T.M. Forte, Characterization of discoidal complexes of phosphatidylcholine, apolipoprotein A-I and cholesterol by gradient gel electrophoresis, Biochim. Biophys. Acta 750 (1983) 353–364.
[42] R.E. Pitas, T.L. Innerarity, R.W. Mahley, Cell surface receptor binding of phospholipid. protein complexes containing different ratios of receptor-active and -inactive E apoprotein, J. Biol. Chem. 255 (1980) 5454–5460.
[43] B. Dehouck, L. Fenart, M.P. Dehouck, A. Pierce, G. Torpier, R. Cecchelli, A new function for the LDL receptor: transcytosis of LDL across the blood–brain barrier, J. Cell Biol. 138 (1997) 877–889.
[44] T.H. Bayburt, J.W. Carlson, S.G. Sligar, Reconstitution and imaging of a membrane protein in a nanometer-size phospholipid bilayer, J. Struct. Biol. 123 (1998) 37–44.
[45] A. Nath, W.M. Atkins, S.G. Sligar, Applications of phospholipid bilayer nanodiscs in the study of membranes and membrane proteins, Biochemistry 46 (2007) 2059–2069.

[46] J. Borch, T. Hamann, The nanodisc: a novel tool for membrane protein studies, Biol. Chem. 390 (2009) 805–814.
[47] T.S. Nguyen, P.M. Weers, V. Raussens, Z. Wang, G. Ren, T. Sulchek, P.D. Hoeprich Jr., R.O. Ryan, Amphotericin B induces interdigitation of apolipoprotein stabilized nanodisk bilayers, Biochim. Biophys. Acta. 1778 (2008) 303–312.
[48] V. Narayanaswami, S.S. Szeto, R.O. Ryan, Lipid association-induced N- and C-terminal domain reorganization in human apolipoprotein E3, J. Biol. Chem. 276 (2001) 37853–37860.
[49] F. Bao, H. Arai, S. Matsushita, S. Higuchi, H. Sasaki, Expression of apolipoprotein E in normal and diverse neurodegenerative disease brain, Neuroreport 7 (1996) 1733–1739.
[50] A.M. Fagan, D.M. Holtzman, G. Munson, T. Mathur, D. Schneider, L.K. Chang, G.S. Getz, C.A. Reardon, J. Lukens, J.A. Shah, M.J. LaDu, Unique lipoproteins secreted by primary astrocytes from wild type, apoE (−/−), and human apoE transgenic mice, J. Biol. Chem. 274 (1999) 30001–30007.
[51] M.F. Linton, R. Gish, S.T. Hubl, E. Butler, C. Esquivel, W.I. Bry, J.K. Boyles, M.R. Wardell, S.G. Young, Phenotypes of apolipoprotein B and apolipoprotein E after liver transplantation, J. Clin. Invest. 88 (1991) 270–281.
[52] J.M. Dietschy, S.D. Turley, Thematic review series: brain Lipids. Cholesterol metabolism in the central nervous system during early development and in the mature animal, J. Lipid Res. 45 (2004) 1375–1397.
[53] M.H. Leung, T.W. Kee, Effective stabilization of curcumin by association to plasma proteins: human serum albumin and fibrinogen, Langmuir 25 (2009) 5773–5777.
[54] A. Barik, K.I. Priyadarsini, H. Mohan, Photophysical studies on binding of curcumin to bovine serum albumins, Photochem. Photobiol. 77 (2003) 597–603.
[55] A.C. Pulla Reddy, E. Sudharshan, A.G. Appu Rao, B.R. Lokesh, Interaction of curcumin with human serum albumin—a spectroscopic study, Lipids 34 (1999) 1025–1029.
[56] C. Castelluccio, G.P. Bolwell, C. Gerrish, C. Rice-Evans, Differential distribution of ferulic acid to the major plasma constituents in relation to its potential as an antioxidant, Biochem. J. 316 (1996) 691–694.
[57] M.T. Huang, W. Ma, Y.P. Lu, R.L. Chang, C. Fisher, P.S. Manchand, H.L. Newmark, A. H. Conney, Effects of curcumin, demethoxycurcumin, bisdemethoxycurcumin and tetrahydrocurcumin on 12-O-tetradecanoylphorbol-13-acetate-induced tumor promotion, Carcinogenesis 16 (1995) 2493–2497.
[58] S.K. Sandur, M.K. Pandey, B. Sung, K.S. Ahn, A. Murakami, G. Sethi, P. Limtrakul, V. Badmaev, B.B. Aggarwal, Curcumin, demethoxycurcumin, bisdemethoxycurcumin, tetrahydrocurcumin and turmerones differentially regulate anti-inflammatory and anti-proliferative responses through a ROS-independent mechanism, Carcinogenesis 28 (2007) 1765–1773.
[59] G.K. Jayaprakasha, L. Jaganmohan Rao, K.K. Sakariah, Antioxidant activities of curcumin, demethoxycurcumin and bisdemethoxycurcumin, Food Chemistry 98 (2006) 720–724.
[60] S. Khanna, H.A. Park, C.K. Sen, T. Golakoti, K. Sengupta, S. Venkateswarlu, S. Roy, Neuroprotective and antiinflammatory properties of a novel demethylated curcuminoid, Antioxid. Redox Signal 11 (2009) 449–468.